

EFFECT OF BLEED SYSTEM ON AIR INTAKE PERFORMANCE

Özgür Harputlu^{*1}, Tekin Aksu¹, M. Tuğrul Akpolat¹, Ezgi Arısoy¹ and Can Çıtak¹
Roketsan Missiles Inc.
Ankara, Turkey

ABSTRACT

Numerical studies are conducted to investigate the performance characteristics of the supersonic intake, considering the effects of the bleed system. In this study, the base model is a two-dimensional rectangular mixed type compression air intake. Numerical simulations are carried out by solving RANS equations with the standard k- ω turbulence model. A parametric study is conducted with different hole inclination angle and the number of holes.

INTRODUCTION

The required air mass flow, i.e. oxygen for combustion, and pressure recovery for supersonic air-breathing propulsion is maintained by air intakes. Air intake performance is of crucial importance in order to maintain a stable combustion. Therefore, one must gain insight on the evaluation of the intake performance. Experimental investigation is a convenient tool regarding the air intake performance. However, it is expensive and resolving three-dimensional flow details which is ubiquitous in an air intake flow path is challenging.

In order to improve the intake performance, one must enhance the boundary layer flow within the inlet flow path. One of the most common ways to do that is to implement boundary layer bleed to avoid high boundary layer thicknesses and/or boundary layer separation which triggers inlet unstart [Herrmann, Siebe, & Gülhan, 2013]. Herrmann et al [Herrmann, Siebe, & Gülhan, 2013] conducted an experimental study comparing air intake performance with and without bleed at Mach numbers between 2.5 and 3.5. The results show that a stable air intake operation with better pressure recovery and mass flow ratio is achieved by employing bleed. The design of bleed in terms of bleed entrance and exit area ratio [Herrman, Blem, & Gülhan, 2011] [Herrmann & Gülhan, 2015], bleed position [Soltani, Daliri, Younsi, & Farahani, 2016], and, bleed slot types, [Bauer & Kurth, 2011] influence of bleed entrance perforation [Bauer & Kurth, 2011] [Fukuda, Roshotko, & Hingst, 1975] are studied by various authors.

¹ Propulsion Systems Design Department, *corresponding author, email: ozgur.harputlu@roketan.com.tr

Boundary-layer separation due to impinging shock waves results in degradation in supersonic inlet performance. Boundary-layer bleed is a commonly used method to eliminate low energy layer near compression surfaces. Bleed acts as a duct system which separates boundary-layer flow from the air-intake. The effect of boundary layer bleed on air-intake performance has been investigated by many research groups by analytical, experimental and numerical methods.

Harloff and Smith developed an analytical model for bleed holes and slots to determine flow rates through bleed system. Their approach includes empirical adjustments for thickness/diameter (L/D) ratio, free stream Mach number and hole angle effects. Predictions of the model was in good agreement with existing test data at different hole angles [Harloff & Smith, 1995].

Domel et al. [Domel, Baruzzini, & Miller, 2012] proposed two separate bleed sections in converging and diverging sections of mixed compression intake, namely performance and stability bleed systems. Performance bleed resides in the converging part and its primary role is to remove low momentum section of boundary- layer and suppress shock-induced separation. Stability bleed is placed in the diverging section and its primary function is to create a stable region for the terminal shock. Bleed ports are modeled as boundary conditions and performance curves are obtained via CFD simulations [Domel, Baruzzini, & Miller, 2012].

Bauer and Kurth examined the sensitivity of air-intake performance on bleed design with wind tunnel tests and CFD calculations. The effect of bleed inlet opening on maximum total pressure recovery, last stable point and stability margin is investigated. Characteristics of intake is obtained both experimentally and numerically [Bauer & Kurth, 2011].

Hermann et al. [Herrman, Blem, & Gülhan, 2011] conducted an experimental work for understanding the characteristics of different boundary-layer bleed systems. They investigated the effect of bleed entrance and exit on pressure recovery, mass flow ratio and stability. Bleed entrance affects the mass flow ratio and stability of shock system. Although having almost no effect on mass flow ratio, bleed exit is found to increase pressure recovery and improve stability point with enlarging exit area. Wind tunnel tests are conducted to find bleed entrance/exit configuration providing the best performance.

Bauer and Kurth [Bauer & Kurth, 2011], emphasize supersonic air intake performance parameters as air mass ratio, total pressure recovery, stability margin and air intake drag. Moreover, air intake drag is divided into four that are spillage drag, cowl drag, friction drag and bleed system drag. Performance of engine is dominated by air intake performance. It is implied that 1 percent total pressure recovery, increases engine thrust by 2 percent.

From past to present, boundary layer control in supersonic flow regimes is substantial topic. In order to control boundary layer, several experiments and numerical studies are conducted. Main approach for boundary layer control is to take bleed air from mainstream. Perforated bleed systems are widely investigated. Before 2000s, perforated bleed systems are studied by experimental methods due to lack of computational power. Willis et al. [B.P. Willis, D.O. Davis, W.R. Hingst, 1995], is carried out perforated bleed system experiments with nine bleed hole configurations with different hole numbers and diameters. Parametric studies are examined with sonic flow coefficient and plenum pressure ratio. Inclined holes enhance flow

coefficient for various plenum ratios. Eichorn et al. [Michael B. Eichorn, Paul J. Barnhart, David O. Davis, Manan Vyas, John Slater, 2013], examine perforated bleed hole configurations on an experimental setup. Parametric study is conducted with different hole inclination angles, hole diameters, hole numbers and hole thickness. Hole inclination angles for experiments are 20, 55 and 90 degrees, hole diameters are changing from 0.794 to 6.35 mm, hole thickness to diameter ratio varies from 0.250 to 2.0. Moreover, number of holes are changing from one to fifteen. In order to examine the performance, for perforated holes best performance is investigated at twenty degree planes with 0.794 mm, fifteen holes.

METHODOLOGY

In this work, a parametric study is conducted to investigate the impacts of different bleed system configurations on the performance of a two-dimensional rectangular air intake. In particular, we changed the hole inclination angle and the number of holes of the bleed system. As shown in Figure1, the former can be defined as the angle between the bottom plane of air-intake and the central axis of bleed holes. It should be noted that all bleed holes have the same inclination angle, as can be seen in Figure1. The first parametric study is carried out to see the effect of the inclination for three different angles with the same hole number. Note that our other work [Citak et al. 2019] emphasizes a method named as the pseudo nozzle model for obtaining a performance map at different back-pressures. Using this method, we obtained performance curves corresponding to six operating conditions for each configuration. The next parametric study focuses on the influence of the number of holes for a superior design. Note that the superior design is obtained based on the findings of the first parametric study. Performance calculations are carried out for three configurations. For details, see the list of design parameters in Table1.

Table1: Bleed Design Parameters

Parametric Study	Configuration Variable	Parameter Values
1	Hole Inclination Angle	45° , 60° , 90°
2	Total Number of Holes	11, 15 ,19

As given, the RANS equations are solved with the aid of a commercial software (FLUENT) and k- ω turbulence model is used to close the Reynolds-averaged conservation equations. Note that the k- ω turbulence for supersonic air intake model is validated based on the experimental findings presented in [Akpolat et al. 2019]. In this paper, a quasi-2D geometrical model for air-intake is studied and therefore, side-wall effects are neglected. A close view of the bleed section is shown in Figure 2. The side planes of the domain are modeled with symmetry boundary conditions. Flow equations are presented in Equation (1), (2) and (3)

$$\frac{\partial \bar{\rho}}{\partial t} + \frac{\partial}{\partial x_i} (\bar{\rho} u_j) = 0 \quad (1)$$

$$\frac{\partial (\bar{\rho} u_i)}{\partial t} + \frac{\partial}{\partial x_i} (\bar{\rho} u_j u_i) = -\frac{\partial \bar{p}}{\partial x_i} + \frac{\partial}{\partial x_j} (\bar{\tau}_{ij} + \bar{\rho} u_j u_i) \quad (2)$$

$$\frac{\partial(\overline{\rho H})}{\partial t} + \frac{\partial}{\partial x_j}(\overline{\rho u_j H}) = -\frac{\partial}{\partial x_j} \left(\overline{\rho \alpha} \frac{\partial H}{\partial x_j} + \overline{\rho u_j H} \right) + \overline{S_H} \quad (3)$$

In order to resolve turbulence Favre averaged flow equations are solved and turbulence related $\overline{\rho u_j u_i}$, $\overline{\rho u_j H}$ and $\overline{\rho u_j Y_M}$ terms need to be modeled. Reynolds stress tensor is defined with Boussinesq approach. According to this approach Reynolds stress tensor is implied as Equation(4).

$$\overline{\rho u_j u_i} = \mu_t \left(\frac{\partial u_i}{\partial x_j} + \frac{\partial u_j}{\partial x_i} \right) - \frac{2}{3} \mu_t \frac{\partial u_k}{\partial x_k} \delta_{ij} - \frac{2}{3} \overline{\rho k} \delta_{ij} \quad (4)$$

Other two term are defined as in Equation(5) and (6).

$$\overline{\rho u_j H} = \frac{\mu_t}{Pr_t} \frac{\partial H}{\partial x_j} \quad (5)$$

$$\overline{\rho u_j Y_m} = \frac{\mu_t}{Sc_t} \frac{\partial Y_m}{\partial x_j} \quad (6)$$

Standard k - ω turbulence model is used for turbulence modeling. Model first introduced by Kolmogorov and simplified by Wilcox [Wilcox, 1998]. Turbulent viscosity is shown in Equation (7).

$$\mu_t = \frac{\overline{\rho k}}{\omega} \quad (7)$$

$$\omega = \max \left[\omega, 0.875 \left(\frac{2\overline{S_{ij} S_{ij}}}{\beta^*} \right)^{0.5} \right] \quad (8)$$

$$\overline{S_{ij}} = S_{ij} - \frac{1}{3} \frac{\partial u_k}{\partial x_k} \delta_{ij} \quad (9)$$

Specific turbulence dissipation rate is shown with ω in Equation (8). At this equation set $\overline{S_{ij}}$ implies averaged strain rate and, β^* denotes turbulence model constant. Turbulence kinetic energy, k , and specific turbulence dissipation rate, ω , is shown in Equation (10) and (11) respectively.

$$\frac{\partial(\overline{\rho k})}{\partial t} + \frac{\partial(\overline{\rho u_j k})}{\partial x_j} = \frac{\partial}{\partial x_j} \left((\mu + \sigma^* \mu_t) \frac{\partial k}{\partial x_j} \right) + \overline{\rho \tau_{ij}} \frac{\partial u_i}{\partial x_j} - \overline{\rho \beta^* \omega k} \quad (10)$$

$$\frac{\partial(\overline{\rho \omega})}{\partial t} + \frac{\partial(\overline{\rho u_j \omega})}{\partial x_j} = \alpha \frac{\omega}{k} \overline{\rho \tau_{ij}} \frac{\partial u_i}{\partial x_j} + \frac{\partial}{\partial x_j} \left((\mu + \sigma \mu_t) \frac{\partial \omega}{\partial x_j} \right) + \sigma_d \frac{\overline{\rho}}{\omega} \frac{\partial k}{\partial x_j} \frac{\partial \omega}{\partial x_j} - \overline{\rho \beta \omega^2} \quad (11)$$

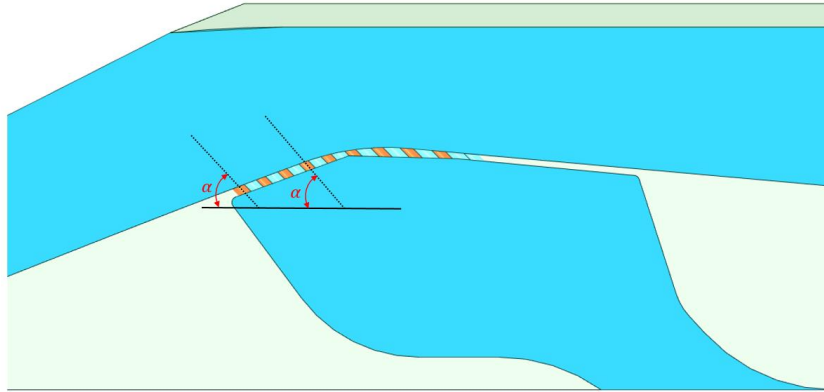


Figure1: Hole Inclination Angle

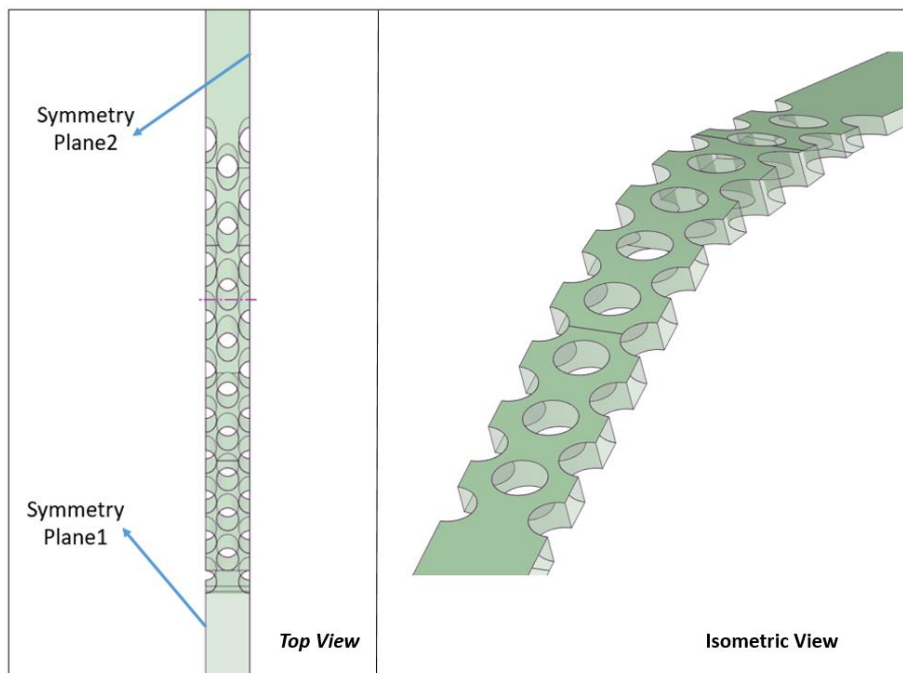


Figure 2: Quasi-2D Bleed Model

In this work, the computational domain is discretized using unstructured tetrahedron cells. The cells in the vicinity of the walls are generated with structured elements to resolve the boundary layer. In a similar manner, a relatively finer mesh is used around the bleed section to capture the mass flow rates more precisely. A plane view of the computational domain is presented in Figure 3.

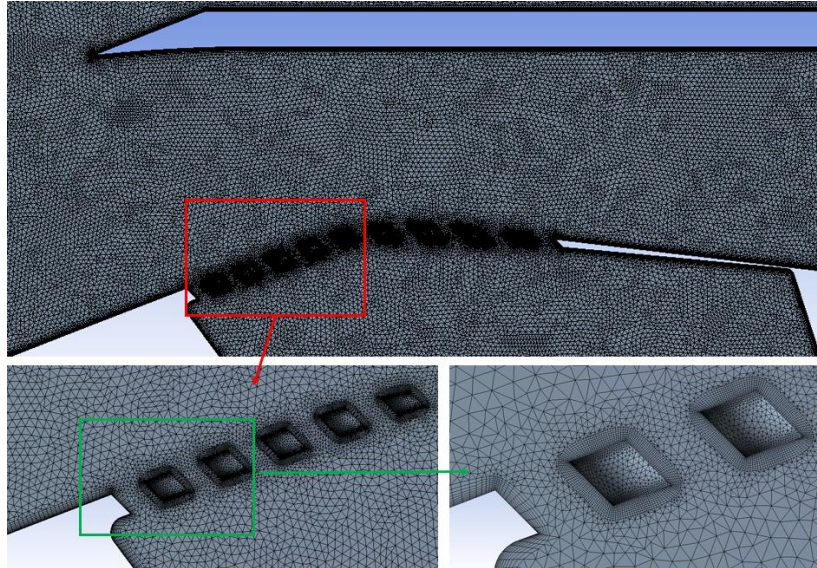


Figure3: Section View of Computational Domain

A refinement study is conducted for the base model with coarse, medium and fine meshes using 1million, 2.4 million and 6.5 million elements, respectively. Results obtained with the three different mesh configurations are compared in terms of the total pressure recovery, mass capture ratio, and the velocity distribution on the indicated lines (see Figure 4 for the six different lines that the data extracted at the mid-plane of the geometry). The performance parameters for the base model with the different number of grid elements are presented in Table 2 and are found to be essentially the same.

$$\text{Total Pressure Recovery (TPR)} = \frac{P_{t\,cc}}{P_{t0}}$$

$$\text{Mass Capture Ratio (MCR)} = \frac{\dot{m}_{cc}}{\dot{m}_0}$$

$$\dot{m}_0 = \dot{m}_{cc} + \dot{m}_{spillage} + \dot{m}_{bleed}$$

Table2: Performance Parameters for Base Model with different meshes

Mesh	MCR	TPR
Coarse	0.7484	0.6862
Medium	0.7477	0.6878
Fine	0.7483	0.6869

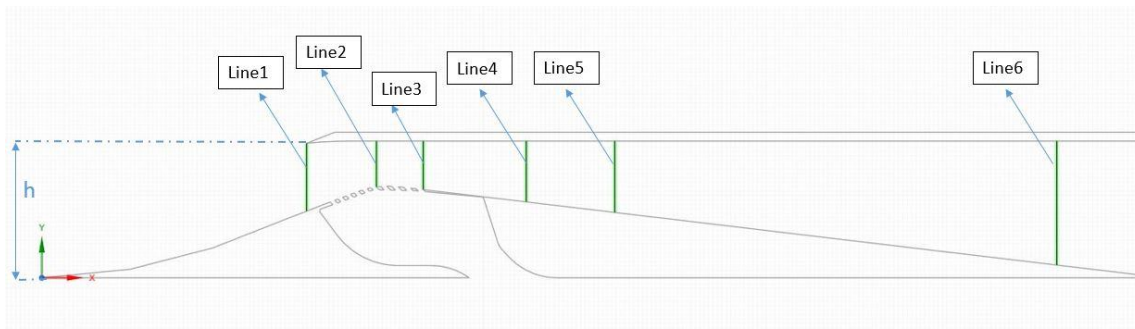


Figure4: The lines where the data extracted for grid convergence study

Total pressure recovery is defined as the ratio of the total pressure of flow at the exit plane of intake to total pressure of freestream flow. Mass capture ratio is the ratio of mass delivered to the combustion chamber to maximum theoretical mass flow rate can enter to air intake's cross section with freestream velocity.

The axial velocity distribution at these six different lines is presented in Figure 5. However, slight differences are observed in the velocity profiles, especially near the throat region. Particularly, the coarser mesh configuration is not capable of capturing the separation region accurately near upper wall of line 4. This phenomenon is important especially in the performance characteristics of the intake at critical places where the terminal shock is located near the bleed region. Since there are no discernible differences between the medium and fine cases, the medium mesh was chosen to decrease the computational cost of the simulations.

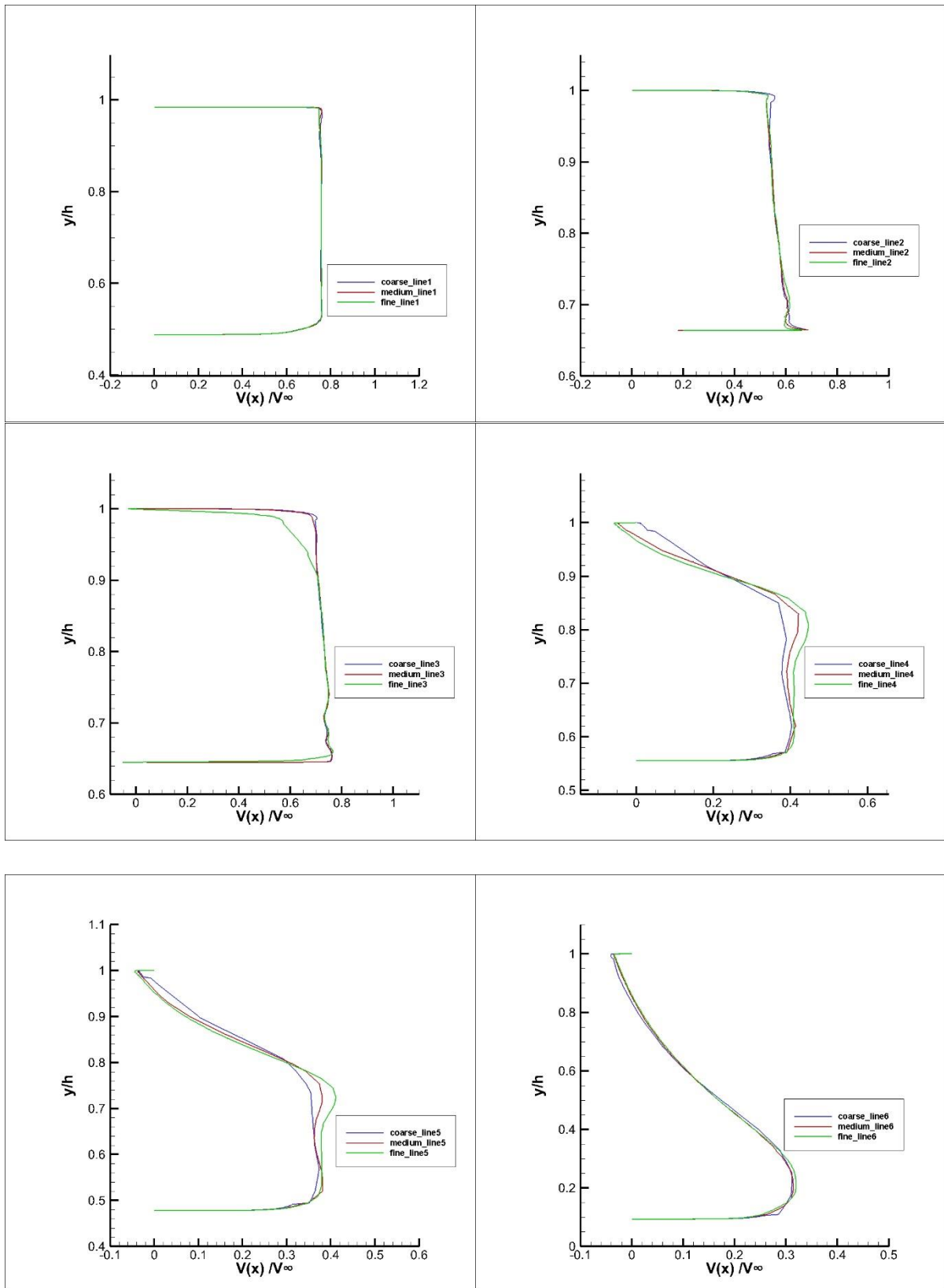


Figure 5: Axial Velocity Distribution on Data Extraction Lines

RESULTS

The effect of hole inclination angle for the configuration with 19 holes is investigated initially. Performance maps are obtained for angles of 45°, 60° and 90°, and results are presented in Figure 6. Performance calculations are limited to last stable operation point where the terminal shock is positioned over bleed section. Any further increase in back pressure results in shock oscillations and therefore an unstable operating regime. Although hole inclination angle does not have a significant effect on maximum pressure recovery, configuration with 45° holes is found to be superior in terms of mass capture ratio. Velocity vector plot and Mach number contour of air intakes having same nozzle parameter but different hole inclination angles, marked in Figure 6, are presented in Figure 7 and Figure 8, respectively.

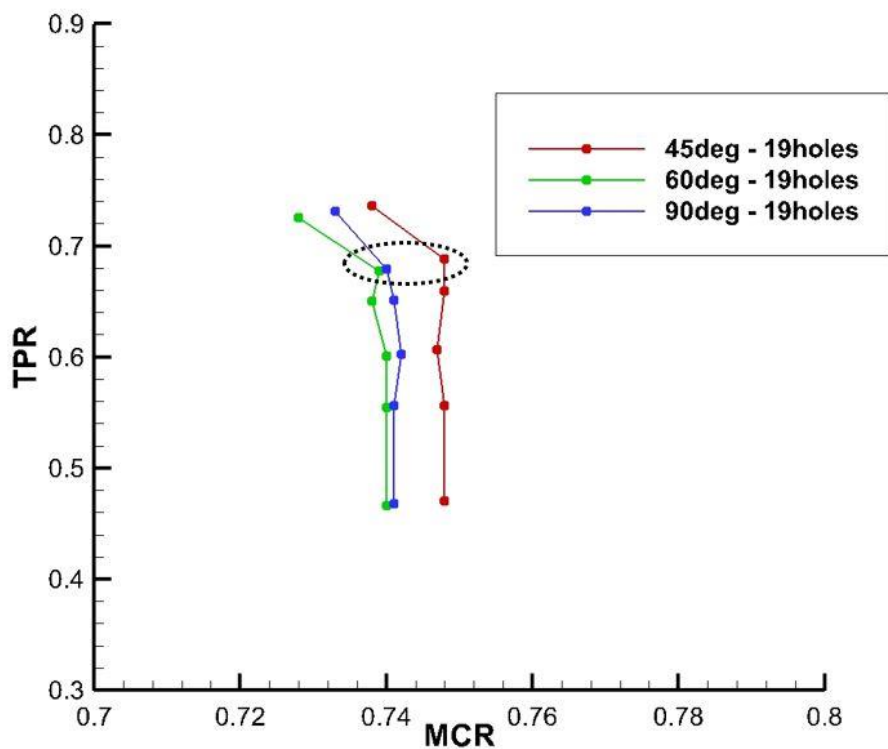


Figure 6: Effect of Hole Inclination Angle on Performance Map

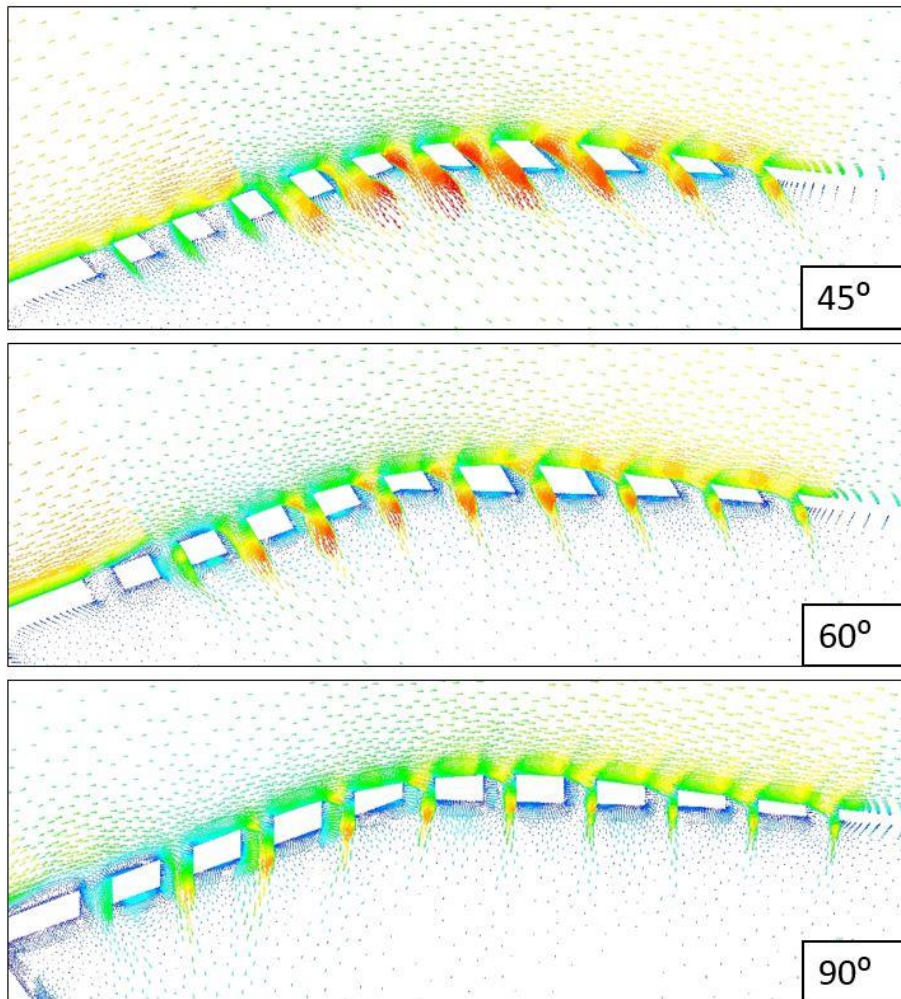


Figure7: Velocity Vectors at Different Hole Inclination Angles

Even if the values of total mass flow rate are in the same order, it is observed that hole inclination angle affects the mass flow rates through individual holes. The varying mass flow rates through individual holes may affect the bleed plenum design. Note that, configuration with 45° holes successfully removes the low momentum layer, while there exists a separation region in 90° model. As the hole inclination angle increases, normal shock near cowl lip moves upstream. Normal shock on third ramp is detached from cowl lip for 90° model which causes additional spillage drag. In case of shock detachment from cowl lip, air intake is prone to buzz operation and pressure oscillations in combustion chamber may result in expulsion of shock system.

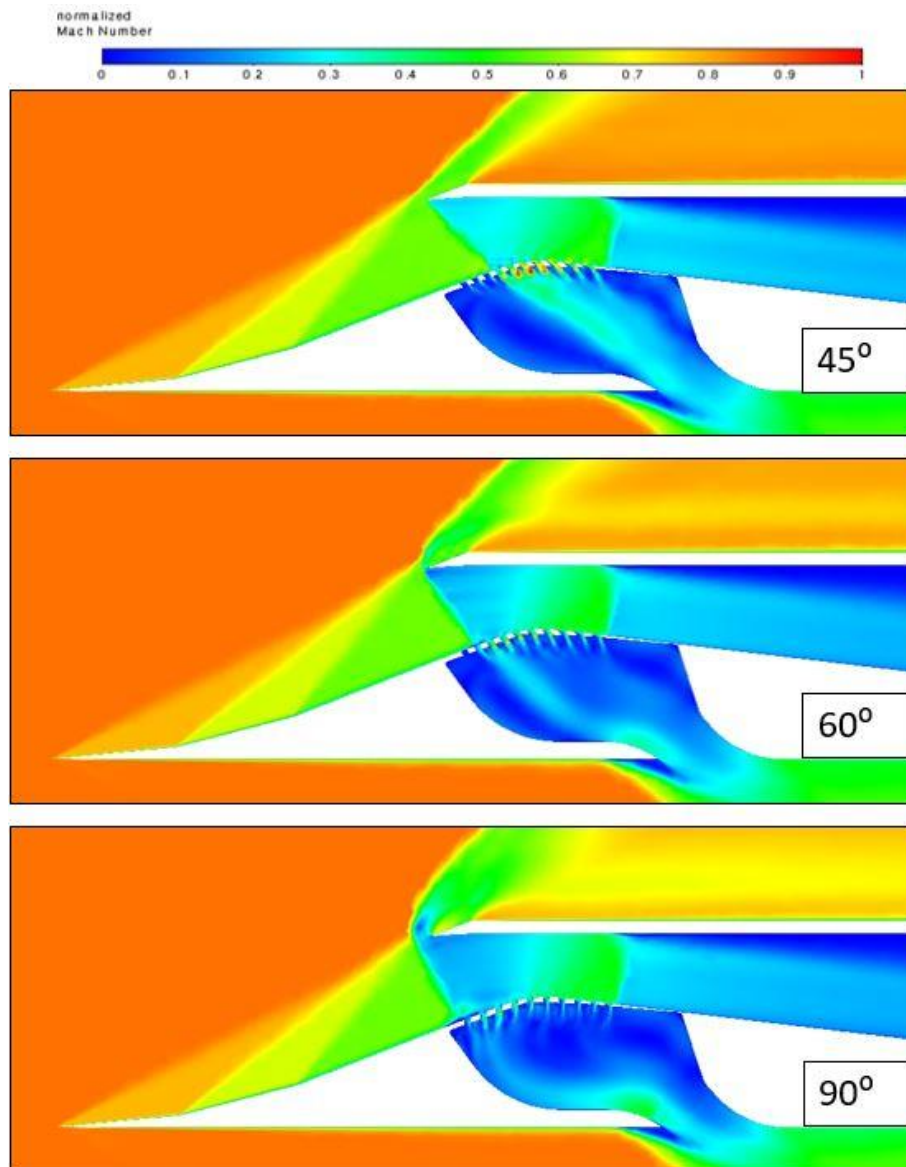


Figure 8: Normalized Mach Contours at Different Hole Inclination Angles

After the hole inclination study, the second investigation focuses on impact of the total number of holes for 45° configuration which is found as a superior model based on the first parametric study. Performance maps are obtained for total number of 11, 15 and 19 holes and results are presented in Figure 9. The results indicate that, as the number of holes decreased, mass flow rate through the bleed section decreases. Therefore mass capture ratio of the air intake increases with decreasing number of holes. Removing bleed holes increases the maximum total pressure up to an extent, any further removal of holes does not provide a marginal increment in terms of TPR limit. These performance results show that an optimization study must be conducted in order to maximize both total pressure recovery and mass capture ratio. Mach number contours for configurations, which is marked on Figure 9, with same nozzle parameter but different hole numbers is shown in Figure 10.

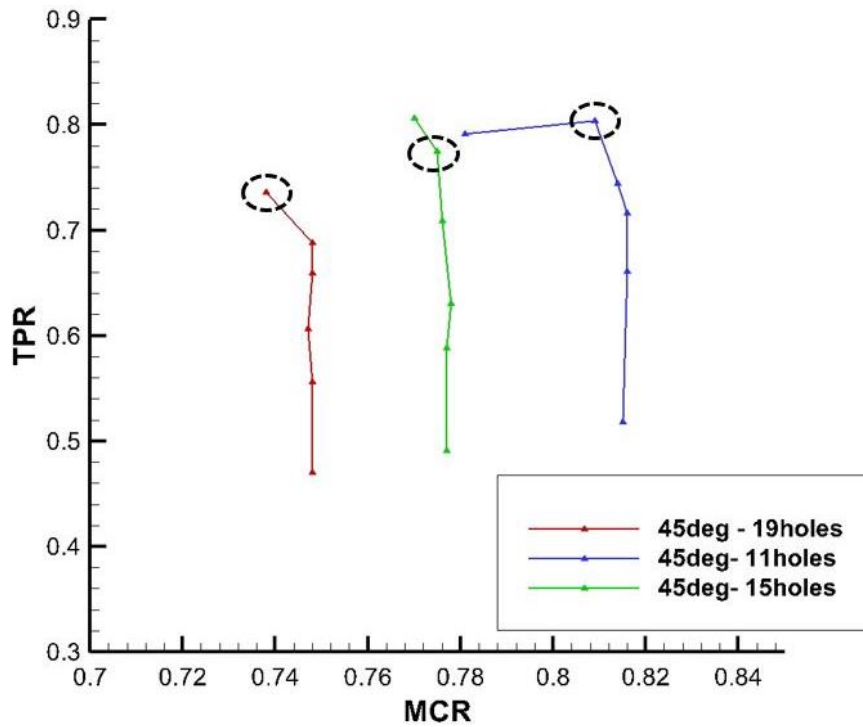


Figure 9: Effect of the Number of Holes on Performance Map

In Figure 10, it can be seen that the location of the terminal shock in the diffuser is varied with the number of bleed holes. The terminal shock moves upstream with decreasing bleed hole number. For the particular case of 19 hole model presented in Figure 10, terminal shock is positioned upstream of last perforation hole and pressure rise due to terminal normal shock increases mass flow rate through this hole. The normal shock position on the third ramp seems not to be affected by the number of holes. The number of holes also has an influence on the flow in plenum and interactions bleed exit jet with freestream. As the bleed system has higher number of holes, mass flow rate ejected to freestream flow increases and this results in stronger interactions at bleed exit region.

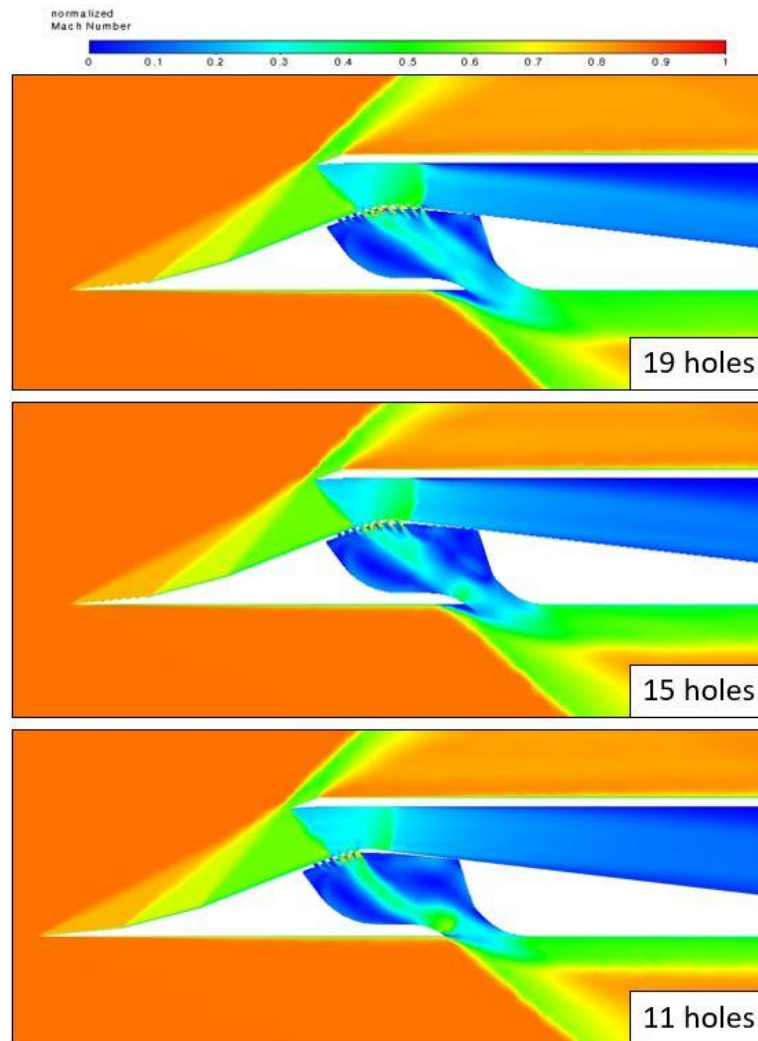


Figure 10: Normalized Mach Contours at Different Number of Holes

CONCLUSION

In this paper, the effect of different configurations of bleed system on the performance of a supersonic air intake is investigated. First parametric study focuses on inclination angle of perforation holes, while the latter one is carried out to see the influence of the number of holes. The impacts of bleed configurations are discussed in terms of performance estimation. It is concluded that both the inclination and the number of the bleed holes may affect the design of the bleed plenum. If the inclination of the bleed holes increased beyond a certain degree the normal shock on the third ramp started to detach from the cowl lip. The number of bleed holes also affect the location of the terminal shock in the diffuser, the terminal shock moves upstream with decreasing bleed hole number. Mass flow regimes through the bleed holes is found to have an impact on flow in the plenum and interaction of exit jet with freestream flow.

References

- Willis B.P., Davis, D.O., Hingst, W.R. (1995). Flow Coefficient Behavior For Boundary Layer Bleed Holes And Slots. 33rd Aerospace Sciences Meeting and Exhibit. Reno, Nevada.
- Bauer, C., & Kurth, G. (2011). Importance of the Bleed System on the Overall Air Intake Performance. 47th AIAA/ASME/SAE/ASEE Joint Propulsion Conference & Exhibit. San Diego, CA: AIAA 2011-5759. doi:10.2514/6.2011-5759
- Das, S., & Prasad, J. (2009). Cowl Deflection Angle in a Supersonic Air Intake. Defence Science Journal, 59(2), 99-105.
- Domel, N., Baruzzini, D., & Miller, D. (2012). A Perspective on Mixed-Compression Inlets and the Use of CFD and Flow Control in the Design Process. 50th AIAA Aerospace Sciences Meeting including the New Horizons Forum and Aerospace Exposition. Nashville, TN: AIAA 2012-0014.
- Eriksson, L., Johansson, U., & Borg, R. (1993). CFD Analysis and Testing on a Twin Inlet Ramjet. AIAA/SAE/ASME/ASEE 29th Joint Propulsion Conference and Exhibit. Monterey, CA: AIAA 93-1839. doi:10.2514/6.1993-1839
- Fukuda, M., Roshotko, E., & Hingst, W. (1975). Control of Shock-Wave Boundary-Layer Interactions by Bleed in Supersonic Mixed Compression Inlets. AIAA/SAE 11th Propulsion Conference. Anaheim, CA: AIAA 75-1182. doi:10.2514/6.1975-1182
- Harloff, G., & Smith, G. (1995). On Supersonic-Inlet Boundary-Layer Bleed Flow. 33rd Aerospace Sciences Meeting and Exhibit. Reno, NV: AIAA 95-0038.
- Herrman, D., Blem, S., & Gülhan, A. (2011). Experimental Study of Boundary-Layer Bleed Impact on Ramjet Inlet Performance. Journal of Propulsion and Power, 27(6), 1186-1195. doi:10.2514/1.B34223
- Herrmann, D., & Gülhan, A. (2015). Experimental Analyses of Inlet Characteristics of an Airbreathing Missile with Boundary-Layer Bleed. Journal of Propulsion and Power, 31(1), 170-189. doi:10.2514/1.B35339
- Herrmann, D., Siebe, F., & Gülhan, A. (2013). Pressure Fluctuations (Buzzing) and Inlet Performance of an Airbreathing Missile. Journal of Propulsion and Power, 29(4), 839-848. doi:10.2514/1.B34629
- Michael B. Eichorn, Paul J. Barnhart, David O. Davis, Manan Vyas, John Slater. (2013). Effect of Boundary-Layer Bleed Hole Inclination Angle and Scaling on Flow Coefficient Behavior. 51st AIAA Aerospace Sciences Meeting including the New Horizons Forum and Aerospace Exposition. Grapevine, Texas.
- Seddon, J., & Goldsmith, E. (1999). Intake Aerodynamics (2nd ed.). Oxford: AIAA.
- Slater, J., Davis, D., Sanders, B., & Weir, L. (2005). Role of CFD in the Aerodynamic Design and Analysis of the Parametric Inlet. ISABE Pağer 1168.
- Soltani, M., Daliri, A., Younsi, J., & Farahani, M. (2016). Effects of Bleed Position on the Stability of a Supersonic Inlet. Journal of Propulsion and Power, 32(5), 1153-1166. doi:10.2514/1.B36162
- Srinivasan, G., & Sinhamahapatara, K. (2017). Large Eddy Simulation of Supersonic Intakes Using Fifth Order Free-Stream Preserving WENO Scheme. 23rd AIAA Computational Fluid Dynamics Conference. Denver, CO: AIAA 2017-3614. doi:10.2514/6.2017-3614
- Trapier, S., Dubeau, P., & Deck, S. (2006). Experimental Study of Supersonic Inlet Buzz. AIAA Journal, 44(10), 2354-2365. doi:10.2514/1.20451

- Citak, C., Harputlu, O., Arisoy, E., Aksu, T. & Akpolat, T. (2019). Computation Methodology Of Performance Characteristics for a Supersonic Air Intake, Ankara International Aerospace Conference
- Akpolat, T., Arisoy, E., Citak, C., Harputlu, O.. & Aksu, T. (2019)., Experimental Validation Of An Air Intake Performance, Ankara International Aerospace Conference
- Wilcox, D., 1998. Turbulence Modelling for CFD. California: DCW Industries Inc..